Plasmon related electrical effects in strongly modulated metasurfaces

D.Keene*, T. Ronurpraful, N.Noginova

Center for Materials Research, Norfolk State University, Norfolk, VA 23504

ABSTRACT

Photogeneration of significant electrical voltages observed in plasmonic metasurfaces is promising for applications in plasmon-based electronics and plasmonic sensors with compact electrical detection. In order to better understand the role of the surface geometry, we study photoinduced electrical effects in profile-modulated plasmonic surfaces. Photoinduced voltages in strongly modulated plasmonic surfaces demonstrate highly asymmetric angular dependence with polarity switching at the plasmon resonance conditions. The effects are attributed to coupling between localized and propagating plasmons and discussed in the frame of the electromagnetic momentum loss approach.

1. INTRODUCTION

The photogeneration of significant electric currents and voltages has been observed in plasmonic films and nanostructures in many studies over the years[1-10]. The strong enhancement of the electrical signals in these studies has been related to the excitation and propagation of surface plasmons. These effects are of interest to both the fundamental physics of light-matter interaction in restricted geometries and in a broad range of practical applications including plasmonic based electronics, fast data processing, and plasmonic sensors with compact electrical detection[11]. While a full theoretical description of these effects eludes the field, systematic experimental exploration is sure to elucidate the search.

The first experiments on plasmon-related electric effects showed the capability to produce significant photoinduced voltages associated with the propagation of a plasmon in the familiar Kretchman geometry[1,2]. The results of these investigations exceeded the predictions of the light pressure model[12,13] by an order of magnitude, even taking into account the enhanced absorption at the resonance conditions[2]. Further studies in nanostructured surfaces show that by employing an array of nano-pilars, even greater voltages could be generated across a sample this time exceeding the predictions of the light-pressure model by orders of magnitude[3]. Also, studies in silver and gold nanomesh and in systems with asymmetric profiles have shown that the polarity of the electrical signals depended not only on light illumination conditions (wavelength, angle of incidence, polarization) but on the nanoscale geometry of the surface features[3-5]. Further studies demonstrated structures wherein the photo-induced voltage can be controlled by varying the ellipticity of the incident radiation[7,9,10,14]. While initial investigations into this phenomenon focused on pulsed laser incidence, more recent work has shown the ability to employ continuous wave systems to tap into the electric response of plasmonic resonances[15].

In all previous studies, the effects were found to be extremely sensitive to nanoscale geometry. In particular, the angular behavior of the photoinduced electrical signal was dependent on the symmetry of the system, and introducing even a slight asymmetry[3] into the sample strongly affected the magnitude of the signal, leading, in some cases, to a complete switch in the electric signal polarity. In an effort to enhance our understanding of the origin of the photoinduced electric signals in nanostructured metal surfaces and the role of nanoscale geometry, we explore the effects in a highly repeatable structure based on mass produced digital versatile disks (DVD's). These samples are easily obtained, requiring only a bit of ingenuity and no specialized equipment. As is discussed below, the photoinduced electrical effects are significant, which show promise in various applications, including low latency opto-electronic interfaces as the conversion of light energy to electric current is purely physical requiring no exciton generation or separation, as in traditional charge coupled devices.

*d.w.keene@spartans.nsu.edu

2. FABRICATION

In order to understand the fabrication process for our samples, one must first understand the structure of the commercially available disks from which the structures considered here are derived. The DVD+R disks we consider consist of four layers; an upper layer of structured polycarbonate (the side that typically has some label attached to it), a metallic reflective layer (in this case silver), a thin coating of photoresist (the writable material), and a bottom layer of structured polycarbonate (the laser incident side of the disk). We have used disks manufactured by Verbatim. The process of creating our samples begins with physically delaminating the disks by prying the layers of the disk apart very carefully. In the ideal case, this results in the metallic reflective layer remaining attached to the top polycarbonate layer. The photoresist is then washed from the resulting two layers by flooding them with methanol. To prevent spotting, each layer is then blown dry with compressed nitrogen. The vast majority of the experiments were done with the manufacturer applied metallic film from the top side of the DVD+R. In addition, a series of samples were crafted using the laser incident side of the disk, in which in house thermal deposition techniques were employed to apply various metal films. In either case this results in a periodic almost square-wave structure with an amplitude in the range of 100-120 nm and a well-defined period of 740 nm. With the upper layer, optical transmission measurements suggest that the thickness

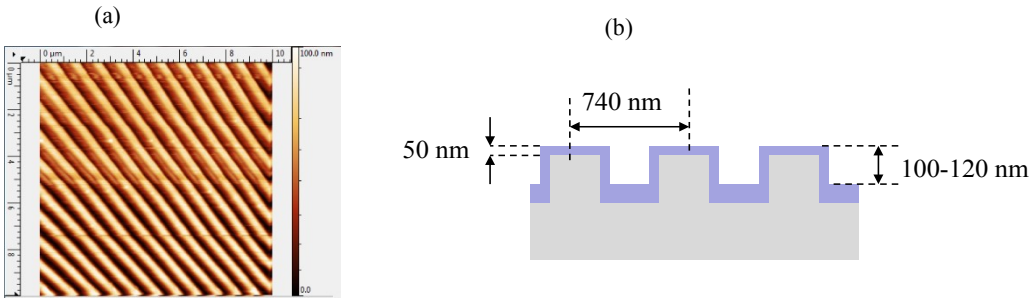

Fig. 1. (a) Atomic force microscopy image of the obtained structure. (b) Schematic of the structure.

of the manufacturer applied metallic film is in the vicinity of 50 nm.

The experimental samples are shown in Figs. 2 (a) and (b). From the chosen side of the disk, a three millimeter long strip is excised radially to obtain a cross-section of the track structure. This serves as the either the substrate to which a metallic film is deposited, or the sample in total depending on the desired final system. This strip is then mounted to a

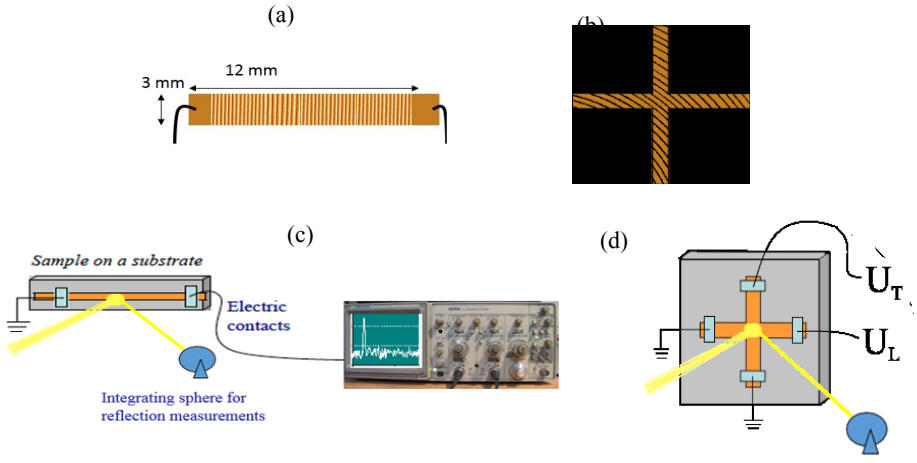

Fig. 2. (a) and (b) Schematics of the experimental samples. (c) and (d) Experimental setup and geometry of the sample orientations.

sample holder with a BNC connector embedded in it to allow for connections to be made to diagnostic equipment. Copper tape is soldered to the terminals of the BNC connecter and each is connected in turn to one of the ends of the completed sample with a binary epoxy impregnated with silver nano-particles to ensure secure electrical connections. These electrical connections allow for the measurement of the voltage disparity across the sample in real time.

Another more complex system (Fig 2 (b)) was also constructed from the same source material. However, in this system instead of excising a simple radial strip the sample was cut in the shape of a plus sign. The resulting samples are mounted such that one set of the arms of the plus sign are oriented horizontally (in the plane of the incident laser) and the other set vertically. Each set of arms is connected to an embedded BNC connector in turn as in the previous set up to allow for the concurrent measurement of electrical signals both longitudinally and transversely. These samples were cut on the bias resulting in a grating vector that is at a 45° angle to both sets of contacts ensuring that the grating vector has approximately equal components parallel to each.

3. EXPERIMENTAL SETUP

After mounting the samples to an apparatus that can be easily connected to an oscilloscope or other diagnostic equipment, the sample holder is then mounted onto a horizontal rotating stage. This allows for the sample to be illuminated with a laser at a controlled angle of incidence, and proper application of mirrors and an adjustable aperture iris allow for control of the light polarization and the incident spot size respectively. The sample is illuminated with pulsed light using the Panther EX+ Optical Parametric Oscillator (OPO) fed by a SureLite III pulsed Nd:YAG laser. The OPO was set to a particular wavelength with an incident power of approximately 5.5 mW. The incident spot size was chosen to slightly exceed the width of the sample. Using a signal from the control box of the Nd:YAG laser as a trigger signal for a Tektronix MSO64 oscilloscope we record the voltage across the sample as it is impacted by the pulsed laser and average that signal over several discharges. The internal resistance of the oscilloscope is set to 50 Ω. An integrating sphere with a photodiode is employed to make reflection measurements concurrent with the electrical measurements to verify that the voltage difference across the sample was indeed the result of plasmonic excitations.

4. EXPERIMENTAL RESULTS

When illuminated by a laser pulse at p-polarization, the samples show a peak in the voltage, as shown in Figure 3 (a). The duration of the electric signal approximately corresponds to that of the laser pulse. In the experiments, the peak magnitude is studied as the function of the incidence angle, θ. Fig 3 (b) shows a typical angular dependence of the peak amplitude obtained in the sample shaped as a long strip (as schematically shown in Fig. 2 (a)). The strongest voltages are observed at small angles, and then, with an increase in the angle of the incidence, they sharply switch their polarity. Here, the negative signal corresponds to electron drag in the direction of the projection of the optical k-vector, k_0. to the sample plane. Illumination at s-polarization produced a much lower signal without prominent features. Thus, below we concentrate on the results obtained with p-polarization.

Note that our sample is basically a plasmonic grating. The surface plasmon polariton (SPP) resonance conditions[16] correspond to the relationship

$$k_{SPP} = k_x + G\ , \tag{1}$$

with $k_x = k_o \sin\theta$, $G = 2\pi/T$, T being the period of the structure, and n, an integer.

The SPP k-vector is estimated as[17]

$$k_{SPP} = \frac{\omega}{c}\sqrt{\frac{\varepsilon_m \varepsilon_d}{\varepsilon_m + \varepsilon_d}}\ , \tag{2}$$

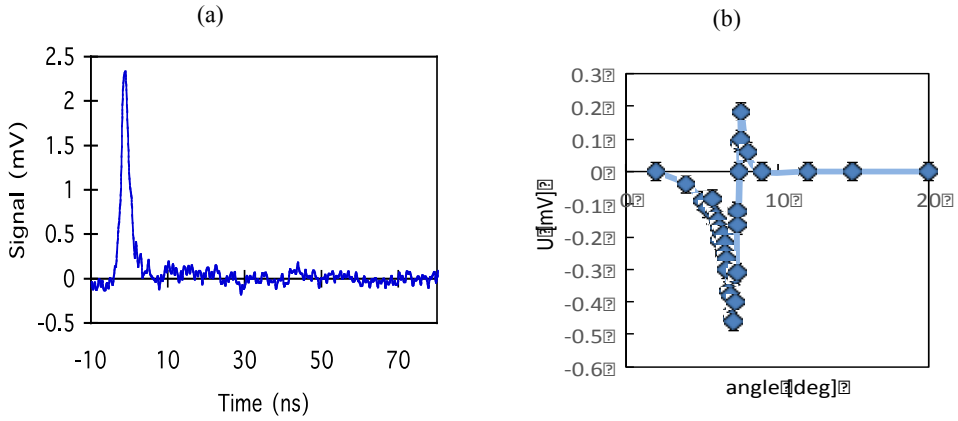

Fig. 3. (a) Typical electric response to the laser pulse. (b) Angular dependence of the signal magnitude at λ = 650 nm.

where ω is the light frequency, and ε_m and ε_d are correspondingly dielectric permittivities of metal and dielectric (air).

Numerical estimations yield the resonance conditions at 8.3 deg. at the wavelength 650 nm, which corresponds to the range of the strongest voltages observed in the experiment shown in Fig. 3 (b). Similar switching is observed at other wavelengths tested (in the range of 530 – 650 nm). In all cases, the switching point approximately corresponds to the SPP excitation condition, which is confirmed by observing the SPP-related dip in the reflectivity profile.

Thus as the angle of incidence is increased toward the SPP resonance condition, the magnitude of the electric current across the sample increases and indicates a flow of electrons in the direction of plasmon propagation. This effect corresponds well to the previous findings[6,8] and theoretical predictions[18,19]. However, upon breaching the resonance condition the electric signal abruptly switches polarity indicating a flow of electrons opposing the propagation of the plasmon through the sample.

This finding is surprising and is not readily predicted with the plasmonic pressure model[18,19]. At this point in the investigation, there was a question as to whether the observed switching phenomenon is driven purely by plasmon propagation or by the interplay between the propagating plasmon and the incident radiation. To test this, we use the plus-shaped sample (with the grooves oriented at 45° with respect to the directions of the arms, Fig. 2 (b)). The electrical contacts allow us to simultaneously record the longitudinal voltage U_L induced in the direction of k_x and transverse voltage, U_T induced in the perpendicular direction.

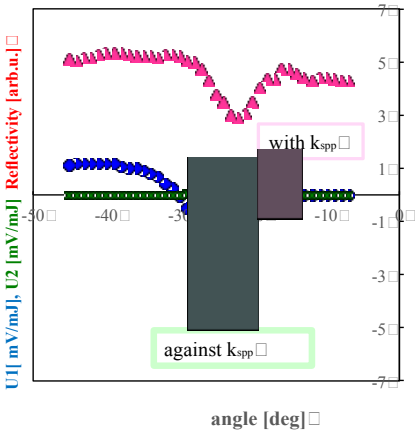

Fig. 4. U_L (blue) and U_T (green) recorded in the plus-shaped sample. Reflectivity is shown in red.

The excitation of the SPP is described with the same Eq (1) but in vector form. The SPP is excited under a certain angle with respect to the direction of k_x. In this case, if the observed switching is due the interplay of incident light and SPP, it will be observed only in U_L.

As can be seen in figure 4, the polarity switching behavior persisted in both the longitudinal (blue diamonds) and transverse (green x's) measurements. The range of the polarity switching corresponds well to the SPP–related to the dip in reflectivity. The fact that the signal presents itself in the transverse measurements, perpendicular to the incidence plane, indicates that the switching behavior is solely a function of the surface plasmons supported by the structure

and not some interaction with the incident radiation.

5. THEORETICAL DISCUSSION

The model under consideration is that of the electromagnetic momentum loss approach[18]. This theory breaks down the differential Lorentz force into two components, a "striction" force composed of the real portions of the constituent components of the Lorentz force and a "pressure" force derived from the imaginary parts of the components of the Lorentz force[8].

$$\bar{f}_{L_i} = \frac{1}{2} Re\{\chi\} \cdot Re\{E_\alpha \partial_i E_\alpha^*\} - \frac{1}{2} Im\{\chi\} \cdot Im\{E_\alpha \partial_i E_\alpha^*\} \tag{3}$$

In the closed circuit regime, the plasmonic pressure force plays the defining role, and predicts an enhancement of the photoinduced electric currents at the conditions of SPP resonance[19]. The effect can also be viewed as linear momentum transfer from the propagating plasmons to the electrons. Since in our gratings the SPP are excited in the direction of k_x, one should expect the drift of electrons in this direction without any change in polarity. On deeper analysis, the similarity between the angular behavior of the voltage disparity across the sample and the Fano resonance line shape is striking. This has led us to suspect the interaction of two resonances as being behind this behavior rather than the expression of a single resonance. This is analogous to the familiar problem of two coupled harmonic oscillators with the change in amplitude of the oscillators corresponding to the change in amplitude of the voltage across the system and the phase change of the oscillators corresponding to the change in polarity of the signal. Let us assume that these two resonances are that of a surface plasmon polariton propagating across the sample and localized surface plasmons that express themselves at the sharp corners of the individual inclusions that make up the structure. To investigate this hypothesis further, a COMSOL model of the system was created. This simulation does indeed confirm the presence of these two distinct phenomena within an overlapping angular incidence range. In Figure 5 (four graphs on the top) one can see the progression of the electric field strength as a function of angle. At low angles, localized surface plasmons express themselves as hot spots on the corners of the structure. As the angle of incidence is increased a propagating plasmon presents itself and dominates the localized plasmons. Increasing the angle of incidence beyond the plasmon resonance condition shows the localized plasmons again beginning to dominate. Within the same model, the pressure forces are calculated according to Eq. 3. Mapping these calculations out on the system as a vector field (Figure 5 bottom) shows that the pressure force at the sharp corners does indeed demonstrate a 180° rotation near the plasmon resonance

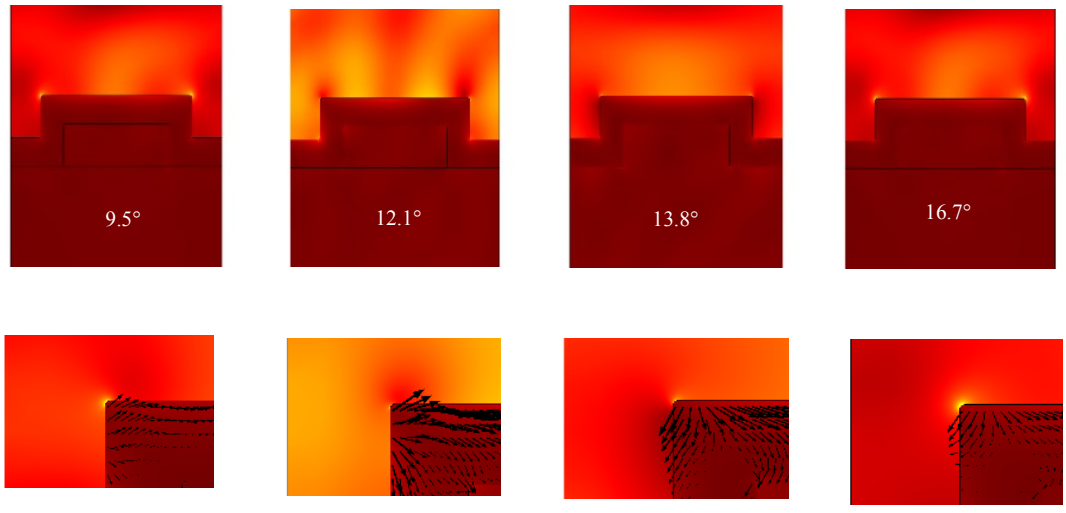

Fig. 5. COMSOL simulations of the electric field strength within the structure considered well before, just before, just after, and well after the plasmon resonance condition (left to right). Below each is an expanded view of the corner of the structure overlaid with a vector field of the "pressure force" derived from the Lorentz force in Eq. 3.

condition. However, in order to explain the polarity switching observed in the experiment, an assumption is required that the contribution of such sharp nanoscale features is dominant in the total photoinduced signal.

6. CONCLUSION

The photo-induced electric signals in plasmonic gratings with a high modulation amplitude demonstrate a highly asymmetric angular dependence with polarity switching from positive to negative voltages. The effects are likely related to coupling between localized surface plasmons and propagating surface plasmon polaritons. Further theoretical analysis is in progress and experimental investigations continue.

Authors would like to acknowledge financial support from National Science Foundation (NSF) (1646789, 1830886); Air Force of Scientific Research (AFOSR) (FA9550-18-1-0417) and Department of Defense (DoD) (W911NF1810472).

REFERENCES

[1] Vengurlekar, A. and Ishiara, T., "Surface plasmon enhanced photon drag in metals," Appl. Phys. Lett. 87(9), 091118 (2005).

[2] Noginova, N., Yakim, A. V., Soimo, J., Gu, L., and Noginov, M. A., "Light-to-current and current-to-light coupling in plasmonic systems," Phys. Rev. B 84(3), 035447 (2011).

[3] Noginova, N., Rono, V., Bezares, F. J., and Caldwell, J. D., "Plasmon drag effect in metal nanostructures," New J. Phys. 15(11), 113061 (2013).

[4] Noginova, N., Rono, V., Jackson, A., and Durach, M., "Controlling Plasmon Drag with Illumination and Surface Geometry," CLEO: QELS_Fundamental Science, # FTh3E. 7 (2015).

[5] Kurosawa, H., Ishihara,T., Ikeda, N., Tsuya, D., Ochiai M., and Sugimoto, Y., "Optical rectification effect due to surface plasmon polaritons at normal incidence in a nondiffraction regime," Opt. Lett. 37(14), 2793-2795 (2012).

[6] Noginova, N., LePain, M., Rono, V., Mashhadi, S., Hussain, R., and Durach, M., "Plasmonic pressure in profile-modulated and rough surfaces," New J. of Phys. 18(9), 093036 (2016).

[7] Ishihara, T., Hatano, T., Kurosawa, H., Kurami, Y., and Nishimura, N., "Transverse voltage induced by circularly polarized obliquely incident light in plasmonic crystals," Proc. SPIE 8461, Spintronics V, 846117 (2012).

[8] Kurosawa, H., and Ishihara, T., "Surface plasmon drag effect in a dielectrically modulated metallic thin film," Opt. Express 20(2), 1561-1574(2012).

[9] Ni, X., Xiao, J., Yang, S., Wang, Y., and Zhang, X., "Photon Spin Induced Collective Electron Motion on a Metasurface," CLEO:2015 , # FW4E.1 (2015).

[10] Akbari, M, Onoda, M., and Ishihara, T. "Photo-induced voltage in nano-porous gold thin film," Optics Express, 23(2), 823-832(2015).

[11] Ronurpraful, T., Keene, D., and Noginova, N., "Electrical Detection of Surface Plasmons for Sensing Applications," CLEO: QELS_Fundamental Science, FTh4C. 7 (2019).

[12] Gibson, A. F., Kimmitt, M. F., and Walker, A. C., "Photon drag in Germanium," Appl. Phys. Lett. 17(2), 75-77 (1970).

[13] Loudon, R., Barnett, S. M., and Baxter, C., "Radiation pressure and momentum transfer in dielectrics: The photon drag effect," Phys. Rev. A 71(6), 063802 (2005).

[14] Bai, Q., "Manipulating photoinduced voltage in metasurface with circularly polarized light," Opt. Express 23(4), 5348-5356 (2015).

[15] Sheldon, M., Van de Groep, J., Brown, A., Polman, A., and Atwater, H., "Plasmoelectric potentials in metal nanostructures," Science 346(6211), 828-831(2014).

[16] H. Raether, [Surface Plasmons on Smooth and Rough Surfaces and on Gratings], 111, Springer Berlin, Heidelberg (1988).

[17] E. Kretschmann and H. Reather, “Radiative decay of non-radiative surface plasmons excited by light,” Z. Phys. 23(12), 2135-2136 (1968).

[18] Durach, M., Rusina, A., and Stockman, M. I., “Giant Surface-Plasmon-Induced Drag Effect in Metal Nanowires,” Phys. Rev. Lett. 103(18), 186801 (2009).

[19] Durach, M. and Noginova, N., “On the nature of the plasmon drag effect,” Phys. Rev. B 93(16), 161406 (2016).